Broadseis: Expectations vs. Achievements

Arun Kumar Behera, Hari K Kanharol, M.K Balasubramaniam*
Reliance Industries Ltd., Mumbai. India

arun.behera@ril.com

Keywords
Broadseis, Deghosting, Broad-source, Variable-Depth Streamer, Boot-strap

Summary

Conventionally acquired seismic data is handicapped by limitations in bandwidth. The last decade or so has seen the industry more focused on addressing the issue with improved hardware and innovative acquisition designs and processing technologies. Ghost free marine acquisition and processing solutions are now the norm with the usable bandwidth reaching to five octaves. One such Acquisition and Processing project was undertaken by Reliance Industries in its lease area in Deep Waters of India through M/s CGG Asia Pacific employing their proprietary Broadseis technology. Here the results achieved post-survey vis-a-vis pre-survey expectations are analyzed and validated with vintage datasets.

Introduction

Broadband seismic wavelet is characterized by its content of both low & high frequencies. High frequencies determine the resolution and low frequencies determine the depth of penetration in addition to enhancing image as well as contributing to inversion stability.

Seismic reflections represented by following convolutional model:

$$T(t)=R(t)*W(t)*S*I + N$$

Where $T(t)$ is a seismic trace as a function of time, $R(t)$ is the reflectivity series, $W(t)$ is the source wavelet, S is the streamer response, I is the recording instrument response and N is the noise. The objective is to record signal with a very wide band of frequencies with minimal noise interference and for this reason the recording hardware must have a large dynamic range as the energy that is not recorded properly cannot be recovered faithfully in any signal processing.

There are two major factors that significantly reduce the bandwidth of the recorded marine seismic data besides the effects of the equipment:
1. Interference between source pulse and reflections from water surface 'ghosts'
2. Earth attenuation (Q)

'Ghosts' are the unwanted reflections from the sea-surface both on source & receiver sides which interfere with the signal and reduce the usable bandwidth. Some frequencies constructively interfere while others destructively interfere producing notches in the spectrum. The notches come at harmonics of frequency $F=Vw/2d\cos\Theta$ where Vw is water velocity, d is the tow depth of source/receiver and Θ is the take-off angle of energy from source.

The tow depth of the streamer determines the frequencies affected. Shallow towing depth compromises the lower frequencies whereas the deep towing affects the higher range of frequencies albeit improving on the lower end. Hence conventional survey acquisition designs always trade-off between the low and high frequencies. The industry is now offering mature technologies to mitigate the impact of this tradeoff and a variety of proprietary solutions are available.

CGG's proprietary solution "Broadseis" is a combination of an innovative source arrangement, curved cable deployment and a deghosting processing scheme. The acquisition designs incorporate multi-level airguns 'Broad source' that compensate for the effect of source-ghosts at acquisition level itself and the variable depth-streamer (8-50m) improves the S/N ratio at low frequency end and provides diversity in receiver notch positions that are effectively tackled and deghosted by the "bootstrap" method in data processing (Wang et al., 2013).

Case study

In year 2014, CGG was contracted to acquire a mid-sized Broadband 3D survey for RIL in its lease area of east coast of India. The area had earlier been covered by conventional seismic as well as a "Q Marine" survey that provided a data set rich in high frequency content (WesternGeco Proprietary). The ghost compensated data set from the Broadseis survey was expected to be the one data set that encompassed a wide range of frequencies from lower end to the higher end of the seismic spectrum. The Pre-survey modeling for fixing acquisition parameters carried out in this case specifically catered to this Broadband campaign and QC process in additional to those used in conventional surveys were implemented to validate the data acquired. The pre-survey theoretical concepts, modeling studies, post-survey data analysis and QC procedures followed in 'Broadseis' acquisition & processing are discussed herewith

Table 1 is a comparison of the acquisition parameters of the three acquisition campaigns in the area. The major changes in Broadseis acquisition as compared to conventional & Q-marine acquisitions are: 1. Multi-level source (Broad-source) 2. Variable-depth streamer (VDS)

Year	Conventional, 2001	Q-marine, 2007	Broadseis, 2014
Source Volume (cu.in)	3147	3147	4630
Source Pressure (psi)	2000	2000	2000
Source Depth (m)	6	4	6 m and 9 m +/- 1.0 m Broadsource
Streamer Type	Digital Nessie-4	Digital N-5 (Q Marine)	Seal Sentinel RD Solid Acquisition Section (SSAS)
Streamer Length (m)	6000	5000	8100
Streamer Depth (m)	8	5	8.0 m to 50 m +/- 1.0 m (Broadseis profile)
Recording System	Triacq 2.1	Triacq V	SEAL 428
High cut filter	200 Hz @ 406 db/Octave	200 Hz @ 477 db/Octave	200(370) Hz (dB/Oct)
Low cut filter	3 Hz @ 18 db /Octave	3 Hz @ 18 db /Octave	2.0(6) Hz (6 dB/Oct) Analogue Digital OUT

Table 1: Acquisition Parameters for three different surveys. Major changes are highlighted in yellow.

1. Multi-level source (Broad-source):

Theoretical expectation of Broad-source optimizing the effect of source-ghost at acquisition level is verified through modelling study. Unlike the conventional acquisition, the air-guns are towed at different depths in such way that by adjusting the firing times for different levels of guns, the primaries are synchronized whereas source-ghosts are de-synchronized (figure 1).

In the mentioned acquisition, two Broad-source arrays are used in 3D flip-flop shooting mode. Each array consists of three sub-arrays (figure 2). All the guns of middle sub-array are placed at a depth of 6m whereas the guns of inner & outer sub-arrays are positioned at depth of 6m and 9m from mean sea-level (MSL). The guns at depth of 9m are fired with a time delay of 2ms to that of 6m guns.

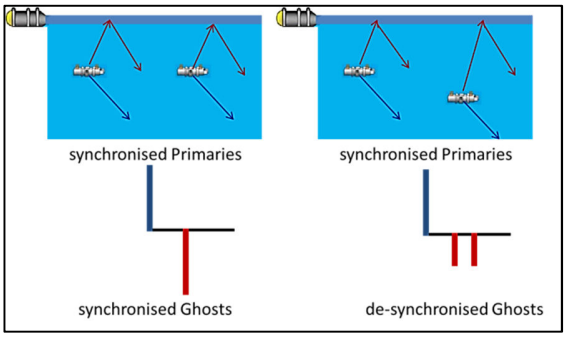

Figure 1: A schematic diagram for conventional and multi-level guns

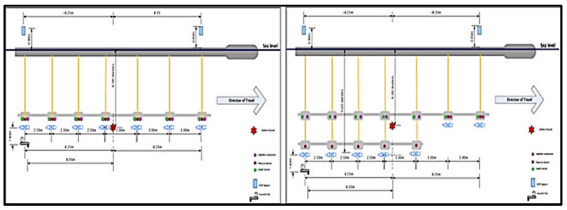

Figure 2: Air-gun positions for mid sub-array (left) and inner & outer sub-arrays (right)

Pre-survey, the far-field signature (FFS) was modeled using Nucleus software and analyzed against conventional design of 6m and 9m of tow depths.

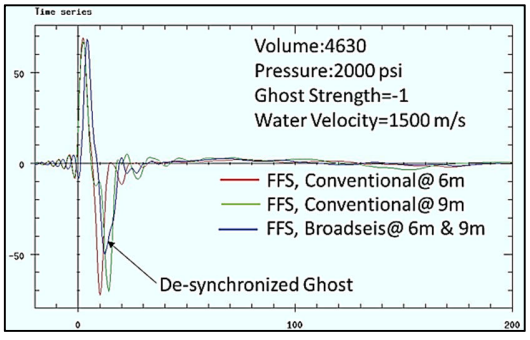

Figure 3: Overlaid FFS for conventional guns at depth of 6m, 9m and Broad-source

The signatures in figure 3 show that the Broad-source exhibit a smaller trough (side-lobe) as compared to the conventional designs.The spectra of the signatures (figure 4) contain sharp ghost notches at 125 Hz & 83 Hz for conventional tow depths of 6m and 9m respectively, where as the Broadsource design is giving a wider spectrum smoothing over the notches.

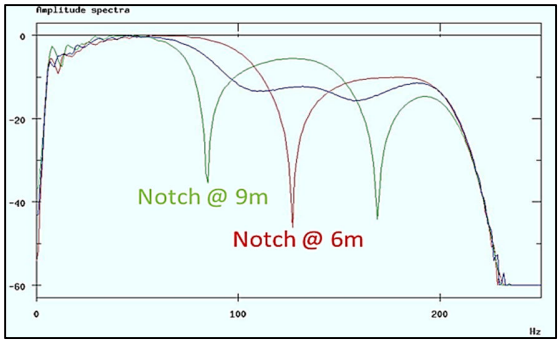

Figure 4: Overlaid spectra for conventional guns at depth of 6m, 9m and Broad-source

In order to validate the achievement against the pre-survey theoretical concepts and modeling results, a FFS was generated from Near-field hydrophone (NFH) records after the survey and compared with the modeling results. NFHs are the hydrophones placed just above some of the selected air-guns in the sub-arrays and shown as pink dots in figure 2. The computation of FFS from NFH is as per the methods described by Ziolkowski, A. et al, 1982 & 1997.

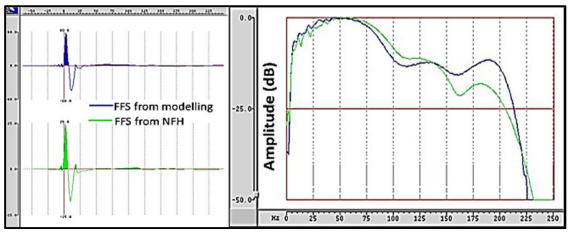

Figure 5: FFS from modeling & NFH (left) and their spectra overlaid (right)

The comparison (figure 5) reveals that the operational source arrays were having almost the same signature as that of the modeled one. Spectra of both exhibit the same behavior without sharp ghost notches. Minor mismatch may be a result of ideal inputs used in modeling study such as: ghost strength=-1, Water velocity=1500 m/s etc.

2. Variable-depth streamer (VDS):

The variable-depth solid streamer acquisitions along with receiver deghost processing not only improve the band-width but also the S/N ratio of the seismic data. Unlike the flat streamer acquisition, the variable-depth streamer acquisition ensures the array is de-tuned with ghost notch frequency varying with depth. After summing the response along the cable, there is no discrete notch and it is possible to access the full bandwidth. The diversity in notch positions plays an important role for proper estimation and removal of receiver ghost through CGG proprietary processing algorithms. So, there is a need to optimize the receiver depth profile in order to ensure diversity for all reflectors depth for a given geological setting and water depth.

In this case, pre-survey modeling was carried out to have an optimized Variable Depth Streamer (VDS) shape. The goal is to have the best notch diversity at all target levels for all offset ranges. On common image gathers, the ghost shape with offset should avoid any horizontal parts, to be optimally cancelled during stack. For this purpose, a 1D reflectivity model is prepared with representative target reflectors and velocities. Synthetics are generated for four Broadseis profiles (8-30m, 8-40m, 8-50m & 10-50m) along with the legacy flat streamer (8m). Migrated gathers, mirror migrated gathers, wavelet with residual ghost and r.m.s residual ghost spectra are analyzed at various targets to finalize the optimum VDS profile (8-50m) for this survey.

Figure 6 shows residual ghost wavelets for all the VDS profiles and conventional flat streamer towed at 8m for target time of 5s. As expected, the wavelet for flat streamer is having a side-lobe of higher amplitude compared to all VDS profiles.

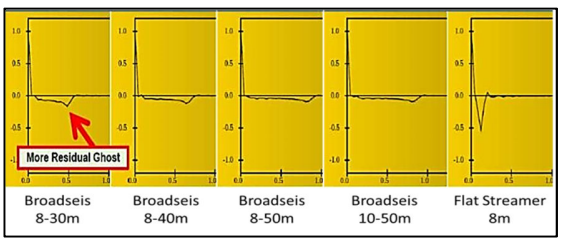

Figure 6: Residual ghost wavelets at 5s target for Broadseis VDS profiles and flat streamer at 8m tow depth

The profile (figure 7) shows a linear slope for first 6km of streamer followed by a horizontal portion of 2km. The first 6km of streamer ensures the notch diversity, while the horizontal portion provides an enhancement of signal below 10 Hz.

It is important to ensure that the depth profile is well maintained throughout the survey. Sercel Nautilus® 3D steering technology used here to maintain the position of the streamer and proper QC procedure followed onboard throughout the survey.

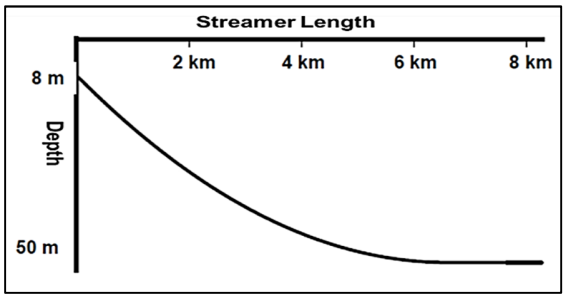

Figure 7: VDS profile (8-50m) used in this survey

Figure 8 shows an arbitrary shot point (SP) for which channel depths are extracted from header values and compared with proposed streamer profile. The operational streamer shape is well matching with the proposed one with an error of ±0.5m.

Post-survey, analyses were carried out on some acquired and processed data to visualize the achievements against the theoretical benefits of using variable depth streamers:

A. S/N ratio increases with tow-depths: The datasets used for this propose are common receiver gathers (CRGs).The positions, depths, offsets of the CRGS are given in the fig 9.

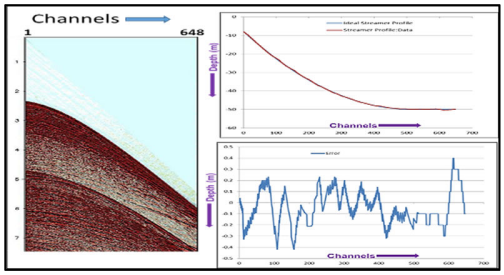

Figure 8: Proposed streamer profile vs. streamer profile from data (top right) & deviation (bottom right) for an arbitrary Shot-point

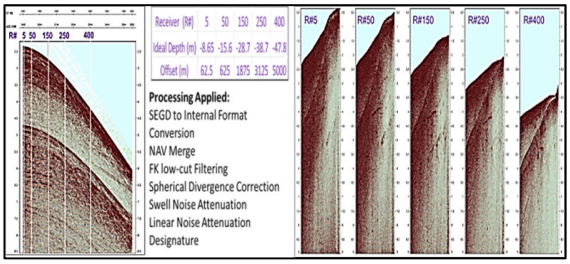

Figure 9: An arbitrary SP (left) showing receiver positions for mentioned CRGs (right) & processing applied

S/N ratios are calculated for the mentioned CRGs over the whole data window and compared. Figure 10 shows a gradual increase of S/N ratio with tow depths significantly at low frequencies.

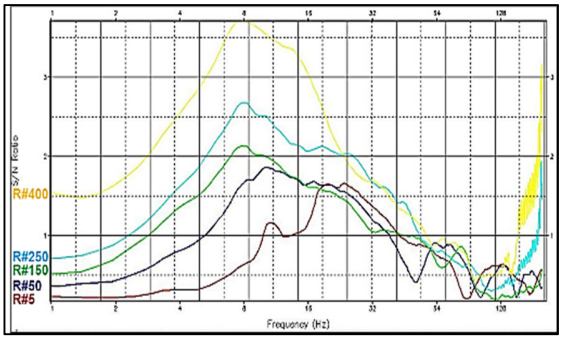

Figure 10: Variation of S/N ratios with tow-depths

B. Notch diversity makes the deghosting algorithm work better to estimate & remove the ghosts: CGG processed the data with pre-migration bootstrap deghosting approach. The bootstrap approach self-determines the required parameters for receiver deghosting. The recorded data are first used to create mirror data through a 1D ray tracing based normal move out correction method. Then both recorded & mirror data are transformed into tau - p domain and are used to jointly invert for the receiver-ghost-free data. Removing receiver ghost before migration provides better frequency response as well as S/N ratio for some preprocessing steps like multiple suppression and velocity analysis.

Figure 11 shows the pre-processing applied to the data before receiver de-ghosting. A rigorous QC procedure was followed generating a number of QC plots and ensuring the proper removal of ghosts.

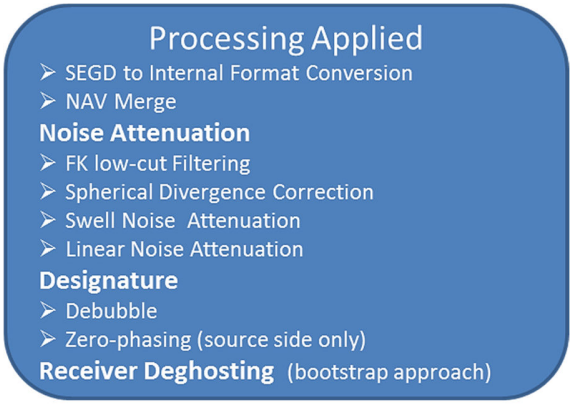

Figure 11: Processing applied to data before receiver deghosting

The following section shows some of the QC plots before and after receiver deghosting. Figure 12 shows a shot-point and analysis window for F-X spectra calculation. The F-X plot before deghosting exhibits notches (shown by arrows) that take the shape of VDS profile & the fill up afterwards.

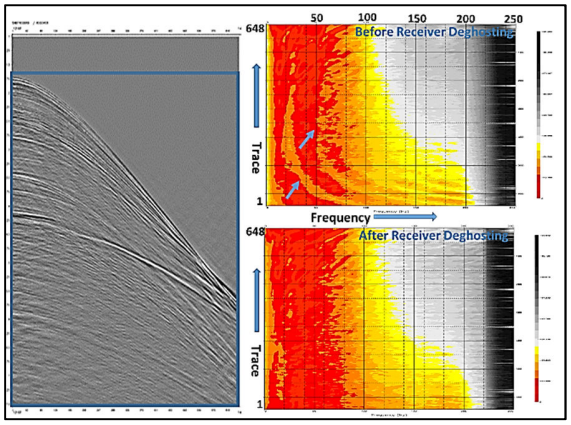

Figure 12: F-X plot before (top right) & after (bottom right) receiver de-ghosting for the shown analysis window of a SP (left)

Another way of verifying the effectiveness of deghosting is to look at the amplitude spectra of CRGs. The figure 13 shows the spectra of four CRGs at different depths shown in figure 9. After deghosting, the ghost notches are properly filled with improvement of both low and high frequencies.

Ghosts behave as short-period multiples that follow the primaries. Figure14 shows NMO corrected gathers & their auto-correlation functions before and after deghosting.

Pre-migration deghosting enables accurate velocity picking, without the challenge of the receiver ghost contaminating the data. Figure 15 shows the improvement in semblance after deghosting.

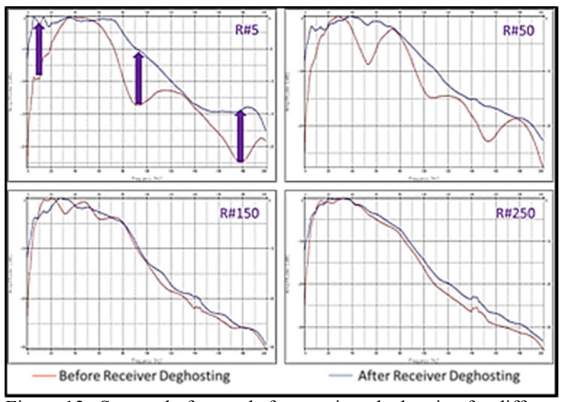

Figure 13: Spectra before and after receiver deghosting for different CRGs

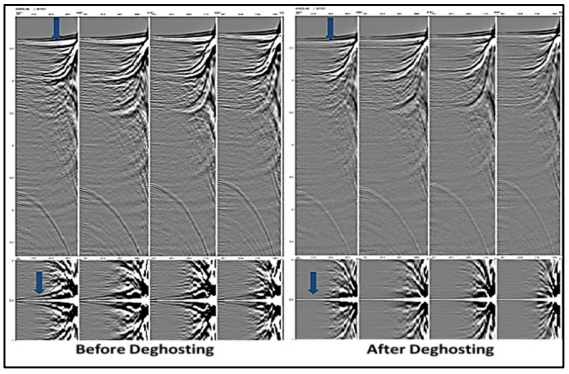

Figure 14: NMO'd gathers (top) & Auto-correlation functions (bottom) before and after deghosting

Phase QC involves checking the phase at the water bottom. Unlike the conventional way, designature is applied here for source-side only with a 1D operator derived from FFS calculated using NFH records. As the data contains both the source and receiver ghosts, it is obvious that it will not be zero-phased after this designature. But after receiver deghosting, the data should be zero-phased. To understand the shape of the WB wavelets at each level, a simulation study is carried out using FFS as shown in figure 16. The FFS contains source ghost only. A zero-phasing operator is calculated & convolved with FFS to get zero-phased FFS (wavelet 3 as shown in left side of figure 16). Now a ghost function is generated and convolved with FFS

to replicate the data before designature (wavelet 1). The operator is convolved with wavelet 1 to get the output wavelet 2 that will be equivalent to the data after designature. So, after receiver deghosting, the data will be properly zero-phased as a replication to wavelet3.

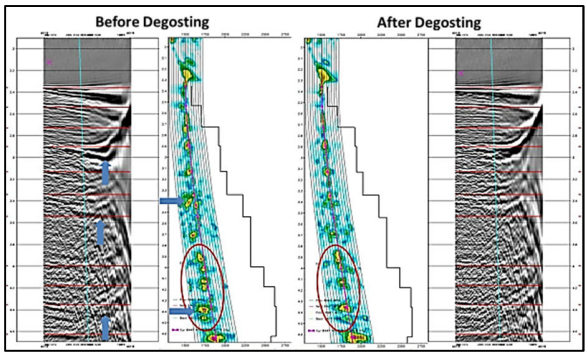

Figure 15: NMO'd gathers & Semblances before and after deghosting

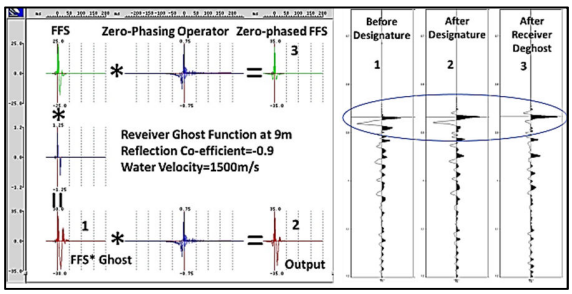

Figure 16: WB wavelets for an arbitrary trace at different stages of processing (right) & simulation understanding using FFS (left)

To verify this, WB wavelet for an arbitrary trace (receiver depth ~9m) is compared at different stages as shown in right side of figure 16. They follow the exact shapes as simulated and the wavelet is properly zero-phased after receiver deghosting. This illustrates the effectiveness of the deghosting algorithm in handling the phase of the data.

Finally, a basic comparison of Broadseis PSTM data is made against the legacy data. In a general sense, the difference in results is a consequence of improved acquisition design and de-ghosting processing.

The figure 17 shows a section with shallow and deeper windows for the spectra analysis.

The Broadseis data shows a wider spectrum (figures 18 & 19) as compared to the legacy data with higher S/N ratios. The low frequency component is considerably improved along with comparable high frequency component. The auto-correlation wavelets have comparatively much lesser side-lobes.

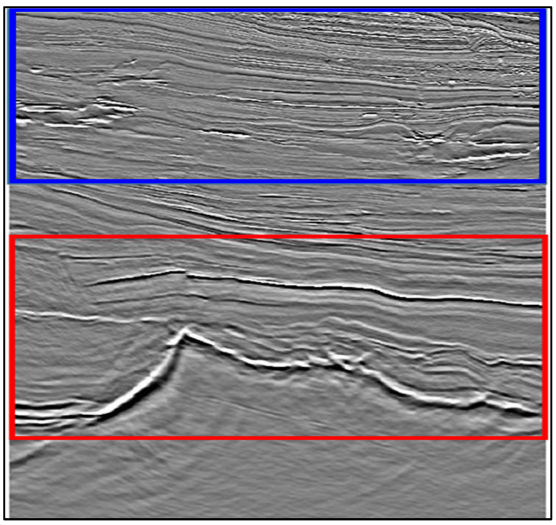

Figure 17: A section showing shallow window (blue rectangle) & deeper window (red rectangle) for spectra analysis

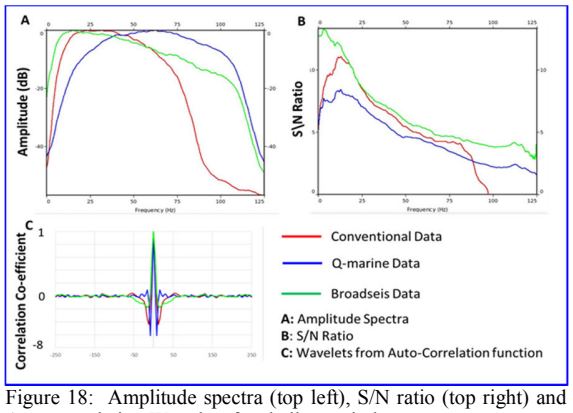

Figure 18: Amplitude spectra (top left), S/N ratio (top right) and Auto-correlation Wavelets for shallow window

Conclusions

Successful adaptation of new technologies involves defining objectives based on theoretical concepts and implementation of the defined workflow supported by relevant QC process.

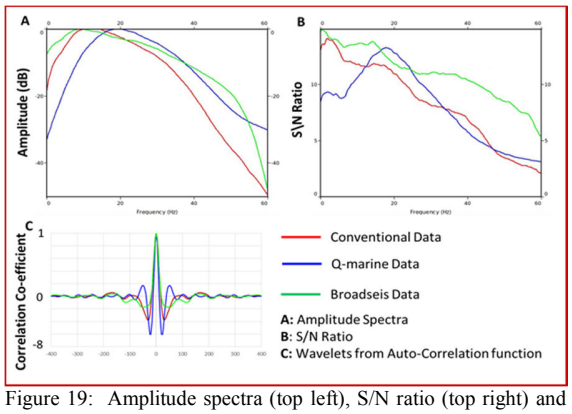

Figure 19: Amplitude spectra (top left), S/N ratio (top right) and Auto-correlation Wavelets for deeper window

Conventional marine seismic data acquired by flat streamer is beset with the ghost problem. A Broadseis project was undertaken by RIL to address and mitigate this problem.

The impact of acquisition design involving Broad-source & Variable Depth Streamer (VDS) profile has been analyzed and conformance to theoretical concepts has been established. Modelling exercises & QC processes were used to validate the results and have been dealt with in this paper.

Overall the Broadseis data has a broader spectrum of frequencies & higher S/N ratio in comparison to legacy data, particularly at low frequency end.

References

Soubaras, R., Dowle, R. and Sablon, R., 2012, Broadseis: Enhancing interpretation and inversion with broadband marine seismic, CSEG Recorder, September 2012

Soubaras, R. and Dowle, R., 2010, Variable-depth streamer- a broadband marine solution, First Break, volme28, December 2010.

Baldock, S., Masoomzadeh, H.,Woodburn, N., Hardwick, A. and Travis, T., 2013, Increasing the bandwidth of marine seismic data, technology: processing, PESA News Resources, April/May 2013

Wang, P., Ray, S., Peng, C., Li, Y. and Poole, G., 2013, Premigration deghosting for marine streamer data using a bootstrap approach in Tau-P domain, SEG Houston Annual Meeting 2013

Soubaras, R., 2013, Optimization of the streamer shape in variable-depth streamer acquisitions, SEG Houston Annual Meeting, Expanded Abstracts 2013

Siliqi, R., Payen, T., Sablon, R. and Desrues, K., 2013, Synchronized multi-level source, a robust broadband marine solution, SEG Houston Annual Meeting, Expanded Abstracts 2013

Ziolkowski , A. , G. Parkes , L. Hatton , and T. Haugland , 1982 , The signature of an air gun array: computation from near - field measurement including interactions : Geophysics , 47 , 1413 – 1421

Ziolkowski, A., and R. Johnston, 1997, Marine seismic sources: QC of the wavefield computation from near - field pressure measurements: Geophysical Prospecting, 45, no. 4, 611 – 639

Acknowledgments

The authors are thankful to Reliance Industries Ltd. for giving them the necessary permissions to present this research paper in the SPG-2017 conference.

Authors are also grateful to Mr. Ram Kripal, Mr. P. K. Srivastava, and Mr. A. K. Biswal of RIL for their continued support and guidance. The efforts of M/S CGG Asia Pacific for acquiring and processing data used in this study are thankfully acknowledged.